

CONSIDERATIONS REGARDING THE CONSTRUCTION OF A MINIROBOT FOR SURVEILLANCE AND INSPECTION

Vlad VADUVA¹, Doru Dumitru PALADE²

In this paper there are presented two designing constructive aspects of a surveillance /inspection mini caterpillar robot. The paper approaches the influence of the wheel-belt assembly on the movement errors and also it approaches the proximal objects detection problem through building sensors characteristics and modeling of ultrasonic sensor placement for optimal triangulation process. Also, for a high detection accuracy and for avoiding some of the triangulation known problems, it was designed a complementary sensor system consisting in a mobile infrared platform.

Keywords: robot, sensors, sensor fusion, mechanical structure, inspection robot

1. Introduction

The designed mini caterpillar robot serves for patrol / inspection in closed premises. The starting location of the robot is considered to be the origin (0, 0) and the spatial coordinates of the necessary inspection points will be scheduled prior to starting. The mini-robot can reach these points in a particular order or for not to be predictable it can be programmed to patrol between these given input coordinates in a random order. The information about the robot real time position is given by actuators encoders, and through the proximity sensory systems the robot is avoiding the obstacles in the path of the patrol. Also, the mini-robot is equipped with sensors to analyze certain key situations in the given patrol points or between them: smoke, hazardous gas, noise, light, for indicating situations like: fire, gas leak, broken pipe, broken window, possible burglary. For each sensor initially there are preselected some values that are considered normal and in the case of exceeding the pre-programmed interval for a sensor the robot triggers an alarm. The preselected values can be standard for the entire route or can be programmed to be different depending on the robot location (for example, in a quiet area of the route, even a little noise can raise suspicions but in a noisy area of the robot path it is required a higher level of noise to raise suspicions). The navigation is made through the potential fields algorithms. The mini robot logical

¹ Eng. National Institute for Mechatronics and Measurement Techniques - INCMDTM Bucharest, Romania, e-mail: vld1985@yahoo.com

² Phd. Eng., National Institute for Mechatronics and Measurement Techniques – INCMDTM Bucharest, Romania, e-mail: palade@cefin.ro

diagram is represented in figure 1 and the designed mini caterpillar robot is shown in figure 2.

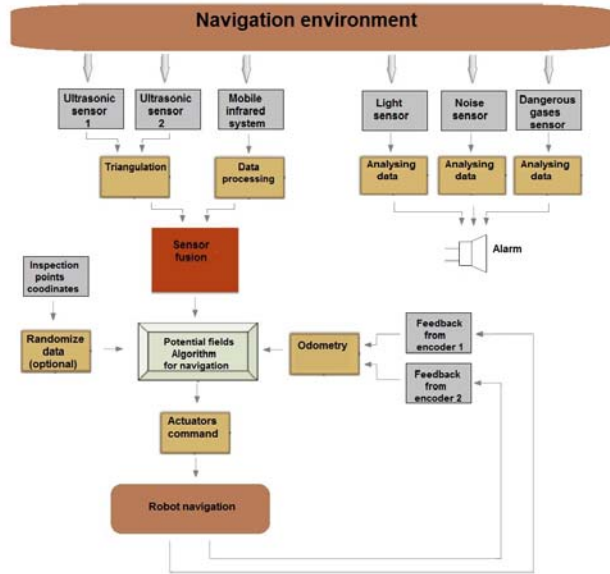


Fig 1. Functional logic diagram of the mini-robot

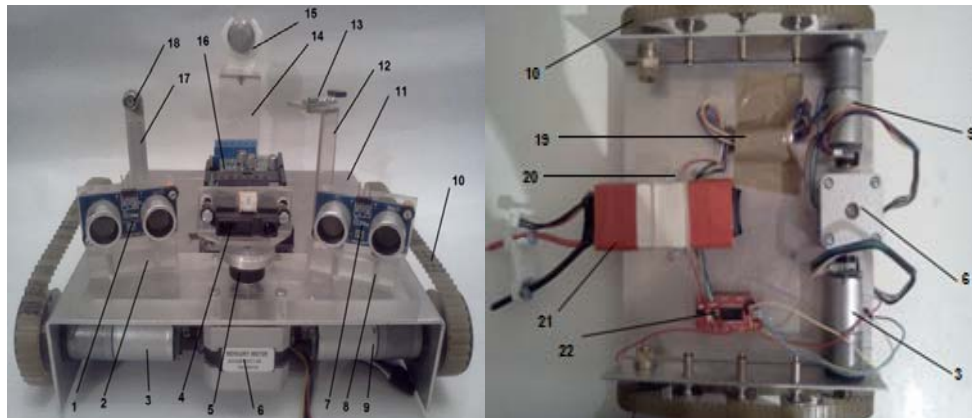


Fig 2. Front and back view of the mini-robot (1-Right ultrasonic sensor, 2-Right ultrasonic sensor support, 3-Right side wheel actuator, 4- Infrared sensor, 5- Infrared mobile platform, 6-Stepper Motor, 7-Left ultrasonic sensor, 8- Left ultrasonic sensor support, 9-Left side wheel actuator, 10-Double toothed belt, 11-Mini-robot case, 12-Light sensor support, 13-Light sensor, 14-Dangerous gases sensor support, 15-Dangerous gas sensor, 16-Electronic command board and actuators driver, 17-Noise sensor support, 18-Noise sensor, 19- Packed wires, 20-Battery Support, 21-Battery, 22-Stepper driver)

2. Influence of the wheel-belt assembly on the movement errors of the robot

At the belt without grooves transmission, where there were used wheels with smooth surface and smooth belt at the contact between the belt and the wheel, during the rotation movement, a sliding occurs between the belt and the wheel expressed in as the elastic sliding coefficient ε [1]. Due to this phenomenon, there is a decrease in peripherals speed of the belt and that leads to decrease in the movement speed of mini-robot, therefore a distance less than the theoretical one. We can write the following equation between the angular movement(or angular speed) of the wheel 1 driven by the actuator and the angular movement of the wheel 2 driven by the belt in the case of a smooth belt [1]:

$$i = \frac{\omega_1}{\omega_2} = \frac{\phi_1/\tau}{\phi_2/\tau} = \frac{\phi_1}{\phi_2} = \frac{D_2}{D_1(1-\varepsilon)} = \frac{n_1}{n_2} \quad (1)$$

i- transmission ratio from the wheel 1 to wheel 2

ω_1 -angular speed of the wheel 1

ω_2 -angular speed of the wheel 2

ϕ_1 -angular movement of the wheel 1

ϕ_2 -angular movement of the wheel 2

τ - time

D_1 -pitch diameter of the wheel 1 corresponding to the diameter of a smooth wheel

D_2 -pitch diameter of the wheel 2 corresponding to the diameter of a smooth wheel

ε - elastic sliding coefficient (in our case 0,015)

n_1 - wheel 1 rotation speed

n_2 - wheel 2 rotation speed

For our designed mini-robot we have:

$D_1 = 38,2$ mm

$D_2 = 20,7$ mm

$n_1 = 130$ rot/min (actuator speed)

n_2 , the wheel 2 speed is given by:

$$n_2 = n_1 \frac{D_1(1-\varepsilon)}{D_2} = 236,3 \text{ rot/min} \quad (2)$$

The wheel 2 speed n_2 is affected by the $(1-\varepsilon)$ factor which takes into account the sliding of the belt

For $\phi_1 = 360^0$ (a full rotation)

$$\phi_2 = \phi_1 \frac{D_1(1-\varepsilon)}{D_2} = 654,4 \text{ degrees} \quad (3)$$

instead of

$$\varphi_{2t} = \varphi_1 \frac{D_1}{D_2} = 664.3 \text{ degrees} \quad (4)$$

So, on a full rotation of the driving wheel 1, the wheel 2 performs a angular movement with almost 10 degrees smaller compared to a transmission with grooves. On 36 theoretical revolutions of the wheel 2, corresponding to a linear movement of the mini-robot

$$L_{36t} = 36\pi D_2 = 2351 \text{ mm} \quad (5)$$

we have performed a real movement

$$L_{36} = 36\pi D_2 (1 - \varepsilon) = 2316 \text{ mm} \quad (6)$$

therefore negative difference of 35 mm which means 1.5%

To compensate these errors we considered two solutions:

1. The number of impulses from the actuators must be multiplied by 0.985, (1- ε) factor, which takes into account the sliding of the belt)
2. This inaccuracy due to the elastic sliding of the belt can be eliminated by using gears with teeth profile specific for toothed belt, in particular with a double toothed belt that will also minimize the sliding at the contact with soil, specifically on shiny surfaces.

Due to the multiple advantages and extra precision for the surveillance /inspection mini caterpillar robot, it has been chosen the second option as a final constructive solution.

In order to test the adopted mechanical solution, we build the robot in a configuration with transmission through belts without interior grooves and with smooth wheels (case 1) and also in a configuration with a double toothed belt and with toothed wheels (case 2). The configuration of the testing room is presented in figure 3, there are defined 3 numbered key points that the robot must reach. Considering the start point coordinates being (0,0) the key points coordinates are presented in table 1 along with the testing results.

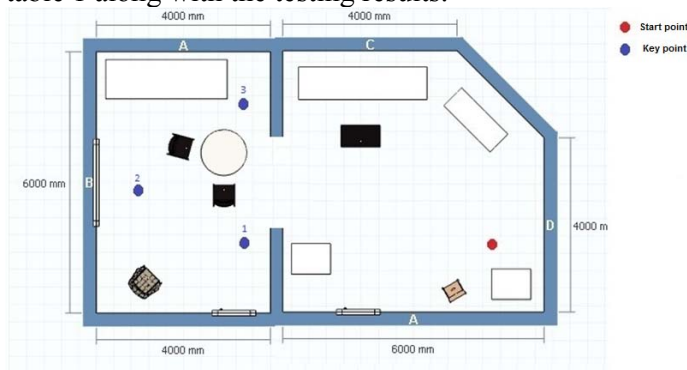


Fig 3. Testing room for the robot

Table 1
Testing results

Key point	Coordinates (mm)	Precision of reaching key points	
		Case 1	Case 2
Key point 1	(5600, 0)	41 mm	13 mm
Key point 2	(8000, 1200)	54 mm	14 mm
Key point 3	(5600, 3200)	58 mm	20 mm

3. Proximal detection system of the mini-robot

For the obstacle detection, ultrasonic sensors were chosen and method of calculating the distance and orientation of the obstacles related to the position of the robot was done by the triangulation method. Triangulation allows us to know precisely the position and angle of which the obstacle found in the common detection zone of two sensors, is positioned related to the robot.

To find out the obstacle distance and angle towards the robot, we need only 2 sensors. In figure 4 is represented the triangulation principle used for the robot

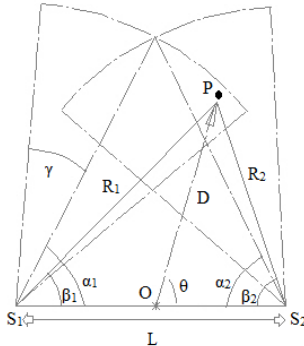


Fig 4. Geometric principle of triangulation (R₁ is the S₁ sensor detected distance, R₂ is the S₂ sensor detected distance, L is the distance between sensors, β₁ is the angle of sensor 1 towards the detected obstacle, β₂ is the angle of sensor 2 towards the detected obstacle, α₁ is the tilt angle of the sensors 1 towards to horizontal, α₂ is the tilt angle of the sensors 2 towards to horizontal, θ is the angle of the detected object towards the central point O, γ is half of the sensors detection cone angle)

According to the geometrical relationship determined by Wijk [2], the equations for the triangulation algorithm are:

$$\cos \beta_1 = \frac{L^2 + R_1^2 - R_2^2}{2LR_1} \quad (7)$$

$$D = \sqrt{R_1^2 + L^2/4 - R_1 L \cos \beta_1} \quad (8)$$

$$\theta = \cos^{-1} \frac{R_1^2 - L^2/4 - D^2}{LD} \quad (9)$$

The disadvantages of triangulation method consists in the appearance of mathematical available solutions but which haven't got a real physical significance like when two distinct objects are detected but one of them is outside of the triangulation area. In this case, the mathematical model interprets it as a single object, incorrectly located related to the real situation [2]. This situation is graphical represented in figure 5.

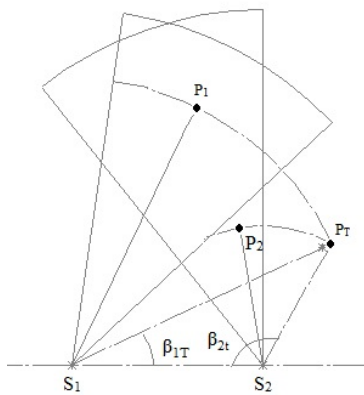


Fig 5. The problem of two objects detected where one of them is in not in the common detection area of the two sensors (P_1 is the object situated in the triangulation area, P_2 is the object that is not situated in the triangulation area and P_T is the mathematical result of the triangulation)

To fix these shortcomings, we should notice that the angles β are located outside the triangulation detection area, so that for the equation 7 we put the condition:

$$\cos(\alpha_1 - \gamma) \leq \cos \beta_1 \leq \cos(\alpha_1 + \gamma) \quad (10)$$

Knowing that $\alpha_1 = \alpha_2$, we observe that the equations are symmetric for both sensors and the limits from the equation 4 apply also for the second sensor [2]

4. Construction of the distance-detection angle characteristic

To perform the triangulation procedure we have conducted a series of tests in order to build the distance-detection angle characteristic of the ultrasonic sensors for the navigation and detection conditions of the mini-robot. The tests were performed under normal operating conditions (temperature, humidity,

luminosity) and at the same height which the sensors will be mounted on the minirobot (7cm).

Because the detection characteristics of the obstacle are different depending on the positioning mode of the obstacles towards the sensors, two tests were conducted. First test was made for the detection of a small parallelepiped object located in a parallel position to the front plane of the sensor and the second test was made with the same small parallelepiped object but with the surface perpendicular to the detection line of the sensor. This cases are graphical illustrated in figure 6.

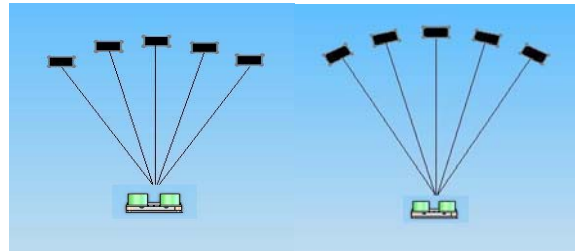


Fig 6. The object positioning mode towards the sensor

The data's that were obtained are listed in table 2.

Table 2

Experimental data regarding the detection limit of the ultrasonic sensors

Distance (cm)	Obstacle positioning towards the sensor			
	Obstacle located in a parallel position to the front plane of the sensor		Obstacle located with the surface perpendicular to the detection line of the sensor	
	Detection limit- left	Detection limit- right	Detection limit- left	Detection limit- right
15	39°	39°	42°	42°
30	28°	28°	39°	39°
45	18°	18°	36°	36°
60	17°	17°	31°	31°
75	9°	9°	22°	22°
90	8°	8°	16°	16°
105	4°	4°	7°	7°
120	2°	2°	2°	2°

First of all, we notice the left and right symmetry of the characteristics. The detection angle gradually increases together with the distance and after reach its maximum, the value decreases until the limit of the detection distance of the object. The largest detection cone is in the case where the object surface is perpendicular to the detection line of the sensor. In figures 7 and 8 the data from table 2 were represented in polar coordinates with the Matlab software.

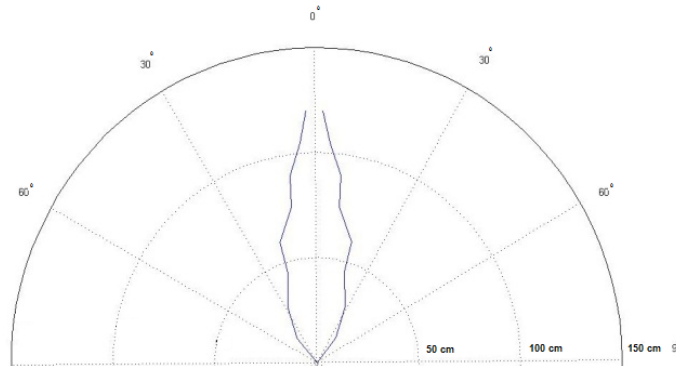


Fig 7. The graphical characteristic of distance-detection angle of the ultrasonic sensors for obstacles located in a parallel position to the front plane of the sensor

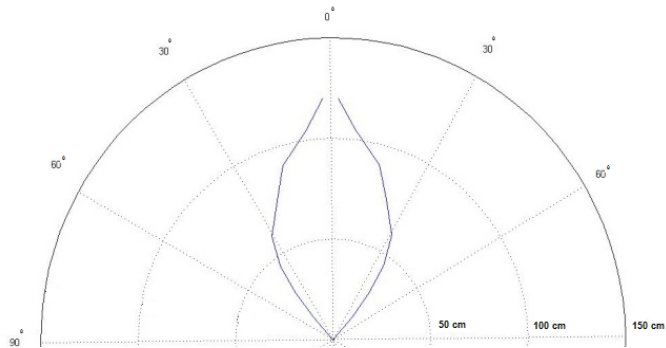


Fig 8. The graphical characteristic of distance-detection angle of the ultrasonic sensors for obstacles located with the surface perpendicular to the detection line of the sensor

5. Modeling of ultrasonic sensor position for triangulation and choosing the optimal inclination angle

The distance-detection angle characteristics calculated in the previous subsection allow us to model the sensor orientation in order to obtain the best position for triangulation. Considering the area where we need the robot to make the triangulation procedure (20-50 cm), we modeled in a CAD software (SolidWorks) the detection cone intersection zone of both sensors. The parameter that indicate us the optimum necessary inclination of the sensors is the common area of the intersection section within the cone of detection of the sensors.

Modeling was done at different angles, starting with 0 to 20 degrees for both cases presented in the previous subsection. In figure 9 it is shown a example of intersection area of the two sensors.

The performed analysis showed us that largest common area of the ultrasonic sensors was found in both cases at 5°. In figure 10 are graphical

represented the triangulation areas for the two cases, between 20 cm and 50 cm at the chosen optimal angle (5°)

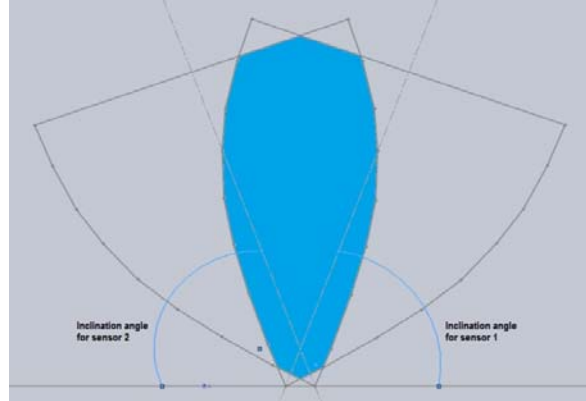


Fig 9. Graphical representation of the whole intersection zone of the sensors made in a 3D CAD software (SolidWorks) from which we selected the region between 20 cm and 50 cm for area calculation

The results of the calculations are listed in the table 3.

Table 3

Areas for common detection zone of the sensors

Degrees	The surface area of the objects located in a parallel position to the front plane of the sensor (mm^2)	The surface area of the objects with the surface perpendicular to the detection line of the sensor (mm^2)
0°	199945	299446
5°	232997	323467
10°	214787	271582
15°	179221	226277
20°	145985	191879

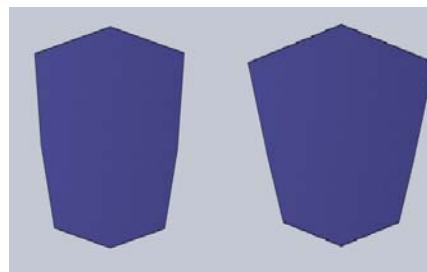


Fig 10. The triangulation areas for the two cases between 20 cm and 50 cm at the chosen optimal angle (5°)

6. Correction auxiliary system for ultrasonic triangulation procedure

For better detection accuracy of the mini-robot and also to be able to detect the object in the triangulation zone correctly in the case where two distinct

objects are detected but one of them is outside of triangulation area, we designed another sensorial system, complementary to the ultrasonic one. The two systems can work individually, but tests conducted have shown the superiority of our detection accuracy in a Fuzzy sensor fusion system.

The designed system consist in a infrared sensor with a incremental angular movement of 30^0 right and 30^0 left mounted in a platform that is controlled by a stepper motor. The infrared sensor is preferable compared to other sensors due to the narrow beam of detection, reaching almost straight line [3]. Also, due to the continuous movement of the platform in which the sensors are mounted we need a quick response from sensors, and the rapid response from infrared sensors (39 ms) [3] makes them perfect for implementation. With this designed mobile platform, we can detected the distance to the obstacle (distance data from infrared sensor) and also the angle in which the obstacle is related to the robot (from the number of steps made by the stepper until the detection)

Also, in order to perform the correction and sensor fusion procedure, it is necessary from the geometric point of view that both sensorial systems to obtain the information, related to the same point of origin (point 0 from figure 4). This system can detect if there are multiples obstacles and some of them are not in the triangulation area, case in which the mini-robot navigation will be based only on data from the infrared system and the ultrasonic system triangulation information are considered wrong and are ignored.

The designed Fuzzy algorithm represented in figure 11 inputs are the sensorial system data (distance to the obstacles, angles of which the obstacles are situated related to the obstacles) and the outputs are the corrected parameters.

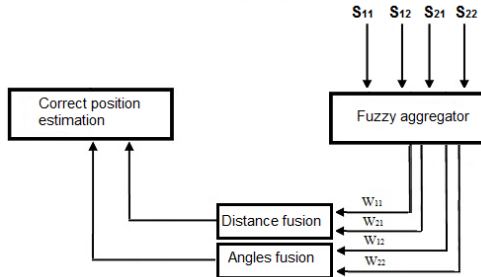


Fig 11. Fuzzy algorithm structure for the mini-robot sensor fusion system (S_{11} the distance detected by the infrared system, S_{12} is the angle of which the obstacle is positioned related to the robot, detected by the infrared system, S_{21} is distance detected by the triangulation ultrasonic system, S_{22} is angle of which the obstacle is positioned related to the robot, detected by the triangulation ultrasonic system W_{11} is the weight of the distance detected by the infrared system, W_{12} is the weight of the angle of which the obstacle is positioned related to the robot, detected by the infrared system, W_{21} is the weight of the distance detected by the triangulation ultrasonic system, W_{22} is the weight of the angle of which the obstacle is positioned related to the robot, detected by the triangulation ultrasonic system)

The confidence level which determines the weights for each sensor on different distances and angles of which the obstacle is positioned related to the robot intervals was established by consulting the technical characteristics of the sensors and by practical precise tests using the precise measurement device F-206.S HexAlignTM 6 Axis-Hexapod for nano-alignment and nano-orientation [4].

Considering f_1 being the function for estimating the measured distance to the obstacle and f_2 being the function for estimating the angle of which the obstacle is positioned related to the robot the equations are [5]:

$$f_1(S_1, S_2) = \frac{S_{11}W_{11} + S_{21}W_{21}}{W_{11} + W_{21}} \quad (11)$$

$$f_2(S_1, S_2) = \frac{S_{12}W_{12} + S_{22}W_{22}}{W_{12} + W_{22}} \quad (12)$$

After we implemented the Fuzzy sensor fusion, we tested all the three detection systems, the results are presented in table 4.

Table 4

Experimental error analysis

	Ultrasonic triangulation system (cm)	Mobile infrared designed system (cm)	Fuzzy logic sensor fusion (cm)
Error Average	0.95	0.76	0.64
Error Dispersion	8.18	4.68	2.01
Standard Deviation	2.86	2.16	1.42

8. Conclusions

The robot was originally built with transmission through belts without interior grooves and with smooth wheels. We did an analysis of the relationships between the angular movement (or angular speed) of wheel 1 driven by motor and the angular movement (or angular speed) of wheel 2 driven by the belt and from the two solutions found, we chose the most precise one.

The tests performed confirmed us the superiority in precision of the system with a double toothed belt. During the experiments we observed that the toothed belt also has several other advantages like minimize the sliding at the contact with soil, specifically on shiny surfaces, and the pre-tension variations in the roller used for tensioning the belt don't affect so much the performance. Also, the mobile robot built with a double toothed belt has a significant advantages compared with a robot driven only by wheels: multi-point contact with ground leading to ability to climb high slopes and to pass over pits.

The modeling of the robot sensory system started with the construction of the distance-detection angle characteristic for the ultrasonic sensors to establish clearly the region of the mini-robot detection. After that, we made the modeling of

the common detection zone of the both sensors through a CAD software and we found the area of the common detection zone for each angular position of the sensors (between 0 and 20 degrees). Following the modeling, we choose the optimum inclination angle (5 degrees).

In the final version of the surveillance and inspection mini-robot, for a high detection accuracy, we built a complementary sensory system consisting in a infrared sensor with a incremental angular movement of 30^0 right and 30^0 left mounted in a platform that is controlled by a stepper motor.

Our test showed that although, each sensory subsystem can provide for the robot navigation precise information regarding the space positioning of the objects, through the tests performed it has been observed that the sensor fusion through Fuzzy method provides a better accuracy.

The advantages of the security robots compared to conventional security systems are: eliminating the human subjective factor (a guard may be tired, distracted or corrupted), patrolling key points can be followed in a random order(a guard can be predictable, with an easy route to see and avoid by a intruder), the robot can inspect certain areas that cannot be entirely viewed by cameras(dead angles), cost efficiency(a robot needs no additional cost after it is programmed for his assignment)

R E F E R E N C E S

- [1] *T. Demian*, "Elemente Constructive de Mecanica Fina" (Constructive elements of fine mechanics), Editura Didactica si Pedagogica, 1980, pp 428-429 (in Romanian)
- [2] *Chris Gearhart, Alex Herold, Dr. Brian Self, Dr. Charles Birdsong, Dr. Lynne Slivovsky*, " Use of Ultrasonic Sensors in the Development of an Electronic Travel Aid ", SAS 2009 – IEEE Sensors Applications Symposium , New Orleans, LA, USA - February 17-19, 2009, pp. 1-3
- [3] GP2Y0A21YK/Sharp Infrared Sensor Datasheet, pp. 1-5
- [4] F-206.S HexAlign™ Manual, General Specifications, pp. 1-5
- [5] *Mohammad Amin Ahmad Akhouni, Ehsan Valavi*, "Multi-Sensor Fuzzy Data Fusion Using Sensors with Different Characteristics", The CSI Journal on Computer Science and Engineering (JCSE), 28 Oct 2010, pp. 1-2.